

Locally Optimal Percolation for Network Resilience Dismantling via Fiedler Vector Gradient Iterative Attack

Kaiming Luo^{1,*}

¹*School of Information Science and Technology, Fudan University, Shanghai 200433, China*
(Received 13 May 2025)

Network resilience, dynamically quantified by the Fiedler value (λ_2 , the second smallest eigenvalue of the Laplacian matrix) ensures functional stability and efficient energy transmission, yet also introduces vulnerabilities that dismantling the resilience of the network can cause a functional breakdown of the network. However, traditional percolation strategies focused on structural attacks often fail to effectively affect resilience and lack universal applicability. Here, we employ a Laplacian spectral perturbation approach to systematically identify and remove edges critical to resilience. We derive the sensitivity of λ_2 to topological changes and employ the gradient of Fiedler vector to measure each edge's contribution of resilience, revealing an intrinsic relationship to community partition. Accordingly, we propose the Fiedler Gradient Iterative Attack (FGIA) algorithm, which constructs locally optimal edge removal sequences to maximize λ_2 degradation with significantly lower computational cost than brute-force methods. Our results offer a rigorous approach for inducing controlled resilience collapse, with potential applications in neuroscience and critical infrastructure protection.

I. INTRODUCTION

The resilience of complex systems encompasses not only functional robustness but also the capacity for rapid recovery and post-disturbance reconstruction[1, 2]. Serving as a fundamental safeguard for mission-critical systems across diverse domains, system resilience inherently coexists with latent functional vulnerabilities. This duality manifests in a variety of scenarios, ranging from neuroscience[3–5] to infrastructure[6–10] and artificial intelligence[11–13], underscoring its cross-disciplinary significance.

Contemporary network attack paradigms predominantly employ percolation strategies that prioritize structural connectivity dismantling[14, 15], typically quantified through the degradation of the largest connected component (LCC). While conventional heuristic algorithms generate attack sequences via network feature-guided node/edge removal, their effectiveness is strongly dependent on network topology and exhibits operational fragility. For instance, degree centrality-based attacks are highly effective against scale-free networks[16] but prove suboptimal for small-world and random topologies. This limitation becomes particularly critical when confronting systems where functional robustness decouples from structural connectivity. This observation highlights the pressing need for universal attack methodologies that transcend specific topological constraints.

A more profound challenge arises from the conceptual divergence between structural collapse and functional disintegration. While LCC adequately measures topological robustness, functional resilience is inherently related to dynamic characteristics encoded in the graph Laplacian spectral properties, particularly the algebraic connectivity quantified by the Fiedler value (λ_2 , the second

smallest Laplacian eigenvalue)[17, 18]. Recent methodological advances have attempted to decompose system functionality through λ_2 -based node[19], edge[20], or cycle[21] criticality analysis. However, such static topology approaches fail to address dynamic functional dependencies, as evidenced by catastrophic infrastructure failures triggered by structurally insignificant perturbations. Furthermore, existing λ_2 -targeting strategies relying on combinatorial search suffer from prohibitive computational complexity (up to $\mathcal{O}(n^6)$), rendering them impractical for large-scale networks. Such spectral correlations invalidate the independent edge contribution assumptions underlying static λ_2 analysis.

In this work, we develop a spectral perturbation approach to mathematically analyze how structural changes in a network influence its resilience, particularly tracking the evolution of λ_2 . Our central discovery reveals that the gradient of the Fiedler vector, which describes how sharply this eigenvector changes across network connections, provides a direct measure of edge importance for maintaining functionality. This gradient-based approach naturally respects eigenvector orthogonality, the fundamental mathematical rule that ensures different eigenvectors remain distinct, thereby preventing interference from other eigenvalues during the analysis.

Accordingly, we propose the Fiedler Gradient Iterative Attack (FGIA) algorithm, a locally optimal edge removal strategy, designed to progressively dismantle a network's resilience. FGIA introduces several key innovations: it utilizes the Fiedler gradient to systematically identify and remove edges that are locally optimal for diminishing network robustness; it ensures the preservation of global network connectivity throughout the sequential edge removal process; and it significantly reduces computational complexity to $\mathcal{O}(n^3)$, achieving exponential efficiency gains over brute-force methods, thereby enabling practical application to large-scale real-world networks.

Through systematic testing on both synthetic networks and real-world infrastructure models, FGIA out-

* kmluo24@m.fudan.edu.cn

performs traditional structure-based attack methods by reducing the required edge removals to achieve equivalent resilience dismantling. Quantitative evaluations using functionality recovery time confirm FGIA's unique position in enabling practical yet potent functional network analysis.

II. RESILIENCE METRIC

An important criterion for measuring network resilience is convergence rate for the system to recover to steady state after being disturbed[22–25]. Consider a steady-state system of n agents with diffusion coupled dynamics. Let $\boldsymbol{\psi}(t) = [\psi_1(t), \dots, \psi_n(t)]^\top$ represents agent states, and let $\mathbf{L} \in \mathbb{R}^{n \times n}$ be Laplacian matrix. The system evolves as:

$$\dot{\boldsymbol{\psi}} = F(\boldsymbol{\psi}) - \mathbf{L}\mathbf{H}\boldsymbol{\psi}, \quad (1)$$

where $F(\cdot)$ describes the intrinsic dynamics, while \mathbf{H} is the inner coupling matrix. Decomposing the initial state $\boldsymbol{\psi}(0) = \sum_{i=1}^n c_i \mathbf{u}_i$, where $c_i = \mathbf{u}_i^\top \boldsymbol{\psi}(0)$, the solution can be expressed as

$$\boldsymbol{\psi}(t) = c_1 \mathbf{u}_1 + \sum_{i=m}^n c_j e^{-\lambda_i t} \mathbf{u}_i, \quad (2)$$

where $0 = \lambda_1 < \lambda_2 \leq \dots \leq \lambda_n$ are sorted eigenvalues and \mathbf{u}_i is the eigenvector, respectively. $c_1 \mathbf{u}_1$ is the stable component while $\sum_{i=m}^n c_j e^{-\lambda_i t} \mathbf{u}_i$ is the dynamical components.

Define the Lyapunov function $V(t) = \frac{1}{2} \|\boldsymbol{\delta}(t)\|_2^2$, where $\boldsymbol{\delta}(t) = \boldsymbol{\psi}(t) - c_1 \mathbf{u}_1$ represents the transient error. Its derivative satisfies:

$$\begin{aligned} \dot{V}(t) &= \boldsymbol{\delta}^\top \dot{\boldsymbol{\delta}} = -\boldsymbol{\delta}^\top \mathbf{L} \boldsymbol{\delta} \\ &\leq -\lambda_2 \|\boldsymbol{\delta}\|_2^2 = -2\lambda_2 V(t), \end{aligned} \quad (3)$$

where the inequality follows from the Rayleigh quotient $\frac{\boldsymbol{\delta}^\top \mathbf{L} \boldsymbol{\delta}}{\|\boldsymbol{\delta}\|_2^2} \geq \lambda_2$. Solving (3) yields

$$\|\boldsymbol{\delta}(t)\|_2 \leq \|\boldsymbol{\delta}(0)\|_2 e^{-\lambda_2 t}, \quad (4)$$

which means the convergence time constant τ satisfies $\tau \sim \frac{1}{\lambda_2}$, with larger λ_2 accelerating network recovery. This fundamental relationship underpins network resilience across physical systems and provides an accurate index which can be quantified for subsequent calculation.

III. MAIN RESULTS

Now we come to consider edge removal specific form by perturbing the Laplacian matrix. Given the intrinsic relationship between network topology and system resilience [26, 27], the removal of edges invariably increases

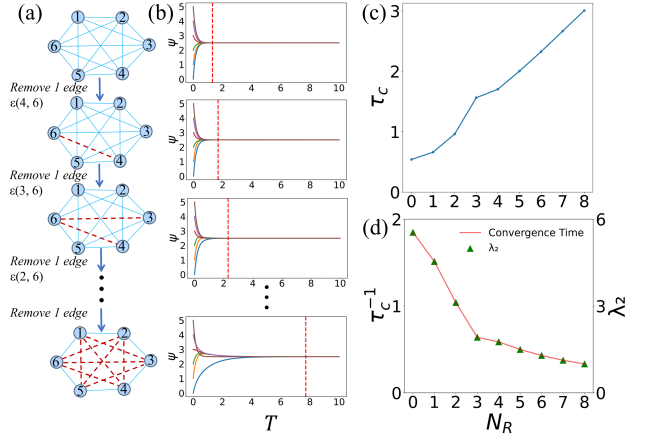


FIG. 1. (a) The generation of edge-attack from an all-connected graph, with the red dashed line representing edges that have been randomly removed. (b) Time Series of dynamics given by Eq. (1) in different graphs in (a), respectively. Black dashed lines mark the convergence time. (c) Convergence time τ_c versus the number of removed nodes. (d) The reciprocal of convergence time (Red dot line) and λ_2 (Green triangle line) versus the number of removed nodes.

the system convergence time, thereby reducing resilience performance [21]. To clearly illustrate the impact of edge attacks on both network connectivity and system dynamics, we apply identical state perturbations across the systems and measure the corresponding convergence times, as shown in Figs. 1(a-c). Moreover, we observe a synchronous variation between the algebraic connectivity λ_2 and $1/\tau_c$, which supports the theoretical prediction in Eq. (4) and is further validated in Fig. 1(d). Collectively, these results confirm that edge removal compromises network connectivity, thereby altering the dynamic characteristics of the system.

Considering edge removal as a perturbation, the eigenvalue equation can be rewritten as

$$(\mathbf{L} + \Delta\mathbf{L})(\mathbf{x} + \delta\mathbf{x}) = (\lambda_2 + \delta\lambda_2)(\mathbf{x} + \delta\mathbf{x}), \quad (5)$$

where $\Delta\mathbf{L}$ to represent perturbation matrix due to edge removal. $\delta\lambda_2$ and $\delta\mathbf{x}$ represent the change in the eigenvalue and eigenvector of \mathbf{L} , respectively. For removal of edge e_{ij} , $\Delta\mathbf{L}(e_{i,j}) = -(\mathbf{e}_i - \mathbf{e}_j)(\mathbf{e}_i - \mathbf{e}_j)^\top$, where \mathbf{e} is the standard basis vector. The eigenvector perturbation $\delta\mathbf{x}$ can be expanded as:

$$\delta\mathbf{x} = \sum_{k \neq 2} c_k \mathbf{x}_k, \quad (6)$$

where \mathbf{x}_k are the k -th eigenvector, satisfying $\mathbf{L}\mathbf{x}_k = \lambda_k \mathbf{x}_k$. Expanding to first order and left-multiplying by \mathbf{x}^\top and considering \mathbf{x} is normalized eigenvector, that is, $\|\mathbf{x}\| = 1$, we have

$$\begin{aligned} \delta\lambda_2(e_{i,j}) &= -(\nabla\epsilon_{ij})^2 \\ &\quad - \sum_{k>2} \frac{(\nabla\epsilon_{ij})^2 (x_{k,i} - x_{k,j})^2}{\lambda_k - \lambda_2}, \end{aligned} \quad (7)$$

where $\nabla\epsilon_{ij} = |x_i - x_j|$ is defined as Fiedler vector gradient, and $x_{k,i}$ is the i -th component of normalized eigenvector \mathbf{x}_k . The first (second) term in RHS is the first (second) order perturbation term. The first term $(\mathbf{x}_i - \mathbf{x}_j)^2$ quantifies the critical relationship between λ_2 and edge gradients in networked systems. Here, the edge gradient directly reflects the information propagation efficiency across the connection, where higher gradients facilitate stronger dynamical coupling and ensure network resilience. Noticing that $\sum_{k \neq 2} \frac{(x_{k,i} - x_{k,j})^2}{\lambda_k - \lambda_2} < 1$, the second term of Eq.(7) can be ignored, which means the rank of edge contribution is totally based on the first term.

Accordingly, we can obtain the objective function for optimal edge removal as

$$Tar(i, j) = \arg \max_{i,j} \nabla\epsilon_{ij}, \quad (8)$$

which identifies optimal edge attacks under connectivity constraints via spectral perturbation theory. By maximizing the nodal difference $\nabla\epsilon_{ij}$ in the Fiedler vector \mathbf{x} , it targets edges bridging the two dynamically heterogeneous modules (positive/negative components of \mathbf{x}). Such edges critically mediate inter-module coordination, where removal maximally degrades λ_2 to dismantle resilience, while preserving global connectivity as these edges are typically non-bridge connections.

To validate this principle, we compare convergence timelines under three distinct interventions in Fig. 2: edge-specific coupling enhancements for the maximum-gradient edge (1, 4), median-gradient edge (4, 5), and minimum-gradient edge (1, 2). The observed convergence time exhibit an inverse correlation with edge gradient magnitudes – the sequence of convergence times aligns precisely with the descending order of gradient values ($\delta\lambda_2^{(1,4)} > \delta\lambda_2^{(4,5)} > \delta\lambda_2^{(1,2)}$). The results demonstrate that gradient-driven edge prioritization effectively captures structural determinants of resilience.

From the perspective of community structure, inter-community edges play a dominant role in synchronization control. Since the nodes connected by inter-community edges exhibit significantly different components in the Fiedler vector, they span a considerable distance in the spectral space. This characteristic not only enhances global coordination but also effectively suppresses phase differences between communities. Removing such edges may lead the originally coherent network to fragment into multiple locally synchronized subsystems, while intra-community edges — with their relatively small component differences — contribute less to the λ_2 , and mainly serve to maintain local synchronization. Their removal may only trigger local oscillations without disrupting overall synchronization.

We further explain this result from the structure of network community. This analysis indicates that the enhanced sensitivity of inter-community edges is primarily due to the steep Fiedler gradient values observed in the Fiedler vector distribution. As shown in Fig. 3, these bridging edges connect nodes with significantly different

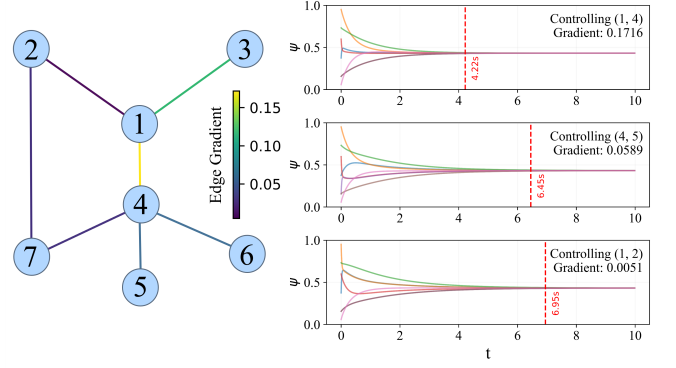


FIG. 2. Status of each node ψ_i , $1 \leq i \leq 7$, versus time t by, respectively, controlling three typical edges based on gradient in the example network, where the edge color represents the gradient, respectively.

eigenvector components. This behavior stems from three main factors. First, structural heterogeneity leads inter-community edges to span regions with different local connectivity patterns, resulting in abrupt transitions in the spectral embedding space. Second, the inherent spectral signature of the Fiedler vector naturally bisects the network, thereby amplifying Fiedler gradients at community boundaries. Third, in the graph's resistive analogy, bridging edges carry a disproportionate amount of current, which is quantified by Eq. (7).

As a result, this disparity in Fiedler gradient values explains the asymmetric impact of edge removal. Removing high-gradient inter-community edges disrupts the spectral bisection balance, causing a significant degradation in the λ_2 and leading to degraded convergence time. In contrast, intra-community edges, which exhibit similar gradient values, have a minimal contribution to λ_2 , making their removal less harmful to resilience.

Therefore, we can degrade λ_2 of the network efficiently by calculating the edge with the maximum gradient as the optimal attack target and ensures that the edge selection results are the same as the violent enumeration method. In many cases, however, we must ensure that the network is connected, while this using Eq. (8) cannot guarantee the connectivity of the network. Therefore, an optimized ranking edge removal algorithm of the Fiedler Gradient Iterative Attack (FGIA) is proposed to ensure the edge optimal attack strategy of the network in the case of connectivity.

As detailed in Alg. 1, systematically disables network edges while preserving global connectivity through (i) spectral bisection, which identifies inter-cluster edges through hierarchical spectral partitioning (Steps 3-5) by computing Fiedler vector \mathbf{x} at each iteration t , (ii) bridge filtering, which employs Tarjan's algorithm (Step 6)[28] to detect and preserve bridge edges, ensuring no critical connections are removed, complemented by gradient ranking based on Fiedler vector differences $|\nabla\epsilon_{ij}|$ (Step 7) and (iii) iterative validation, which performs progres-

Algorithm 1: Fiedler Gradient Iterative Attack (FGIA)

Input : Network $G = (V, E)$, attack budget k , bisection depth d_{\max}
Output: Attack edge sequence E_{attack}
Initialize: $E_{\text{attack}} \leftarrow \emptyset$, $G^{(0)} \leftarrow G$
for $t \leftarrow 0$ **to** $k - 1$ **do**

1. Compute Laplacian $\mathbf{L}^{(t)}$ of $G^{(t)}$
2. Solve Fiedler pair $(\lambda_2^{(t)}, \mathbf{x}^{(t)})$
3. **Hierarchical Spectral Bisection**:
 $l \leftarrow 1$
while $l \leq d_{\max}$ **do**
 Partition $G^{(t)}$ into $\{G_1^{(l)}, G_2^{(l)}\}$ via $\text{sign}(\mathbf{x}_i^{(t)})$
 Extract cross edges
 $E_{\text{cross}}^{(l)} \leftarrow \{e_{ij} \mid v_i \in G_1^{(l)}, v_j \in G_2^{(l)}\}$
 if $|E_{\text{cross}}^{(l)}| < 0.1|E^{(t)}|$ **then**
 break ; // Adaptive pruning
 $l \leftarrow l + 1$
4. **Gradient sensitivity Ranking**:
 Compute $\nabla \epsilon_{ij}$ for all $e_{ij} \in E_{\text{cross}}^{(l)}$
5. **Bridge Detection**:
 Find all bridge edges B in $G^{(t)}$ using Tarjan's algorithm
6. **Edge Filtering**:
 $E_{\text{non-bridge}} \leftarrow E_{\text{cross}}^{(l)} \setminus B$
 if $E_{\text{non-bridge}} = \emptyset$ **then**
 break ; // No removable edges, terminate attack
7. **Edge Ranking**:
 Sort $E_{\text{non-bridge}}$ by $\delta \lambda_2$ in descending order ;
 // Ranking based on $\nabla \epsilon_{ij}$
8. **Iterative Connectivity Validation**:
 for $m \leftarrow 1$ **to** $|E_{\text{non-bridge}}|$ **do**
 Select $e^* \leftarrow$ the m -th edge in sorted list
 Create $G_{\text{temp}} \leftarrow G^{(t)} \setminus \{e^*\}$
 if G_{temp} is connected **then**
 break ; // Found edge preserving connectivity
9. **Update State**:
 $E_{\text{attack}} \leftarrow E_{\text{attack}} \cup \{e^*\}$
 $G^{(t+1)} \leftarrow G_{\text{temp}}$
 $\mathbf{L}^{(t+1)} = \mathbf{L}^{(t)} - (\mathbf{e}_i - \mathbf{e}_j)(\mathbf{e}_i - \mathbf{e}_j)^\top$

return E_{attack}

sive edge removal from the sorted candidate list until confirming network connectivity preservation (Step 8).

In terms of complexity, the practical efficiency of FGIA algorithm is derived from a combination of optimized computational strategies. The process begins with an initial Laplacian spectrum decomposition, which has a complexity of $\mathcal{O}(n^3)$. Following this, the algorithm performs iterative updates of the Fiedler vector using the inverse power method, contributing a complexity of $\mathcal{O}(kn^2)$. Additionally, an adaptive spectral bisection is carried out over $k \times d_{\max}$ layers, resulting in a complexity of

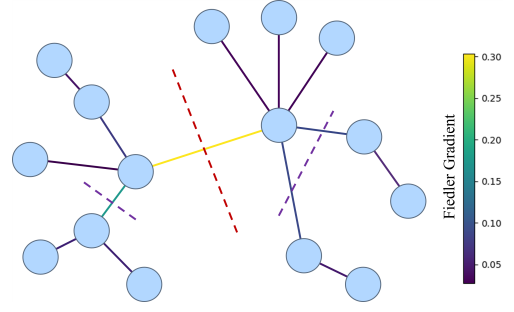


FIG. 3. Diagram of community partition and the Fiedler gradient. a demonstrative case in a Barabási–Albert (BA) network with 15 nodes and attachment parameter $m = 1$. The color bar shows the Fiedler gradient. The red dotted line represents the first partition, and the purple dotted lines represent the second partition.

$\mathcal{O}(k d_{\max} m)$, and the algorithm employs a linear-time bridge detection (via Tarjan's algorithm) with a complexity of $\mathcal{O}(km)$. Combined, these steps yield an overall complexity for FGIA of

$$\mathcal{O}(n^3 + k(n^2 + d_{\max} m)).$$

In contrast, a brute-force method would require the evaluation of all $\binom{m}{k}$ possible edge combinations, with each combination involving an eigenvalue computation at a cost of $\mathcal{O}(n^2)$. This leads to a total complexity of $\mathcal{O}(\binom{m}{k} n^2)$. For limiting case, considering the extreme case of a complete graph, FGIA algorithm maintains a scalable complexity of $\mathcal{O}(n^3)$. However, even when $k = 2$, the brute-force approach escalates dramatically to $\mathcal{O}(n^6)$, thereby clearly illustrating the significant scalability advantage of FGIA algorithm over traditional brute-force methods.

Notice that, in Fig. 4(a-f), when the value of pER exceeds a certain threshold, the FGIA algorithm may exhibit a noticeable change in the AUC degradation rate. It indicates that continuing to remove edges based on the criterion defined in equation (8) may result in network disconnection. To prevent this, Alg. 1 adopts a degradation strategy based on the Fiedler gradient sequence of edges, thereby preserving the network's connectivity. Although this modification introduces additional computational complexity, we argue that ensuring connectivity while assessing network resilience is of significant value.

However, if users opt for an attack strategy that does not require preserving network connectivity based on the network's functionality and attack objectives, then the bridge detection (Step 5), edge filtering (Step 6), and connectivity verification loop (Step 8) in Algorithm 1 can be omitted. Moreover, by modifying the ordering constraints (Step 7) so that the sorting extends from being applied solely to bridge edges to covering all inter-partition edges, we obtain a degenerate version of Alg. 1. Although this version does not guarantee network connectivity, it is more destructive and achieves improved efficiency.

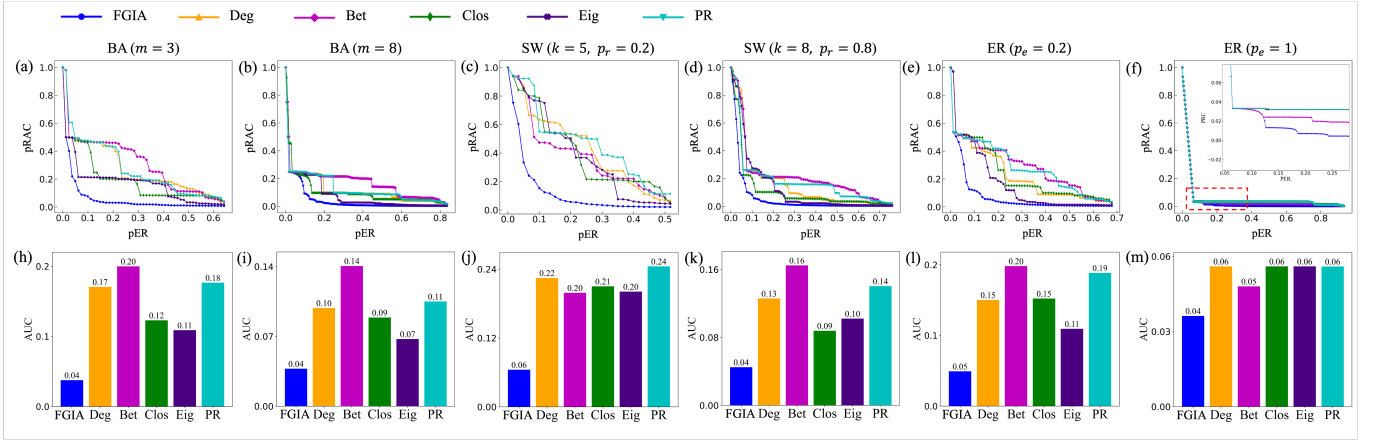


FIG. 4. The performance of various dynamical edge-attack algorithms on resilience of synthetic networks is illustrated in the top row, quantified by the resident percentage of λ_2 (pRAC) as a function of the percentage of edge removal (pER). The results are based on synthetic network models comprising 30 nodes. The effectiveness of each attack strategy is further assessed using the area under the curve (AUC) of λ_2 . (a) and (b) correspond to Barabási–Albert (BA) scale-free networks, (c) and (d) to Watts–Strogatz (WS) small-world networks, and (e) and (f) to Erdős–Rényi (ER) random networks. The inset in (f) provides an enlarged view of the region highlighted by the red dashed rectangle. The bottom row displays the corresponding AUC values for each method, aligned with the plots in the top row. The bar chart in (h-m) shows the AUC values obtained by different algorithms in the first row.

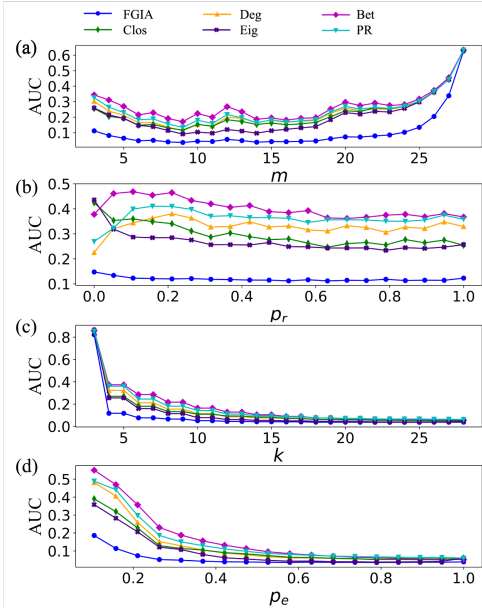


FIG. 5. The AUC values obtained from several representative attack algorithms across different synthetic network models. (a) In Barabási–Albert (BA) scale-free networks, AUC values are plotted against the network growth parameter m . (b) and (c) show the results for Watts–Strogatz (WS) small-world networks: in (b), AUC values vary with the rewiring probability p_r (with average degree fixed at $k=5$), and in (c), with k (with fixed $p_r=0.3$). (d) presents the results for Erdős–Rényi (ER) random networks, with AUC values shown as a function of the edge connection probability p_e . Different colors represent different attack algorithms, as indicated in the legend.

IV. SIMULATION AND ANALYSIS

To illustrate the accuracy of FGIA algorithm, a comparison result in synthetic network, including Barabási–Albert (BA), Erdős–Rényi (ER) and Watts–Strogatz (WS) networks with different generation parameters, are shown in Fig. 4(a–f). We systematically evaluates the performance against conventional edge-removal algorithms across synthetic networks with distinct topologies. The metric of λ_2 —normalized as the percentage residual algebraic connectivity (pRAC)—is plotted against the percentage of edges removed (pER) to quantify network resilience. In addition, we quantify functional dismantling capability with the area under curve (AUC) of λ_2 degradation, where a smaller AUC corresponds to superior performance.

As evidenced in Fig. 4(h-m), FGIA consistently achieves the lowest AUC values among all evaluated algorithms—including degree based (Deg), betweenness centrality based (Bet), closeness centrality based (Clos), eigenvector centrality based (Eig), and PageRank based (PR) attack algorithm (for the two nodes of the corresponding edge)—validating its dominance in functional network disruption. A notable edge case arises in near-fully connected Erdős–Rényi (ER) networks (edge probability $p_e=0.8$), where initial structural homogeneity marginally limits FGIA’s early-stage performance. However, as the edge removal ratio exceeds 5%, emergent heterogeneity enables FGIA to exploit spectral phase gradients, achieving a conspicuous lower AUC than competitors shown in the inset of Fig. 4.

Notably, the efficacy of compared algorithms vary significantly depending on network-specific characteristics.

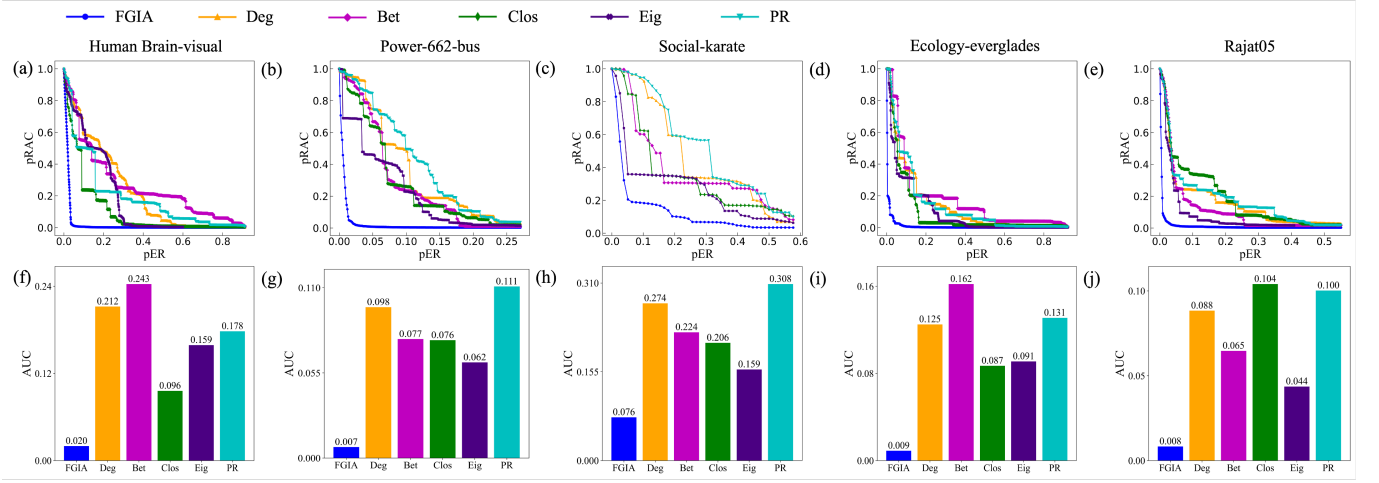


FIG. 6. The interpretation follows the same convention as described in Fig. 4, but applied to some typical real-word networks in different domains.

For example, closeness centrality (Clos) shows relatively competitive performance in the SW ($k=5$, $p_r=0.8$) network in Fig. 4(d, k), while it fails to generalize to the SW ($k=5$, $p_r=0.2$) network in Fig. 4(c, j) or ER ($p_e=0.1$) network in Fig. 6(f, m). On the contrary, all the results highlight FGIA’s adaptability that its gradient-driven spectral analysis bypasses the limitations of topology-dependent heuristics, ensuring universal superiority regardless of network size, density, or functional context.

Further, to rigorously assess universality, we systematically scan network parameters across 100 independent realizations in Fig. 5. The result reveals that FGIA maintains a consistent AUC advantage over all benchmarks, even in extreme clustering regimes. These results confirm FGIA’s parameter-agnostic robustness, establishing it as a universal strategy for resilience dismantling in both heterogeneous and homogeneous networks.

These results underscore FGIA’s broad applicability and robustness across diverse network types, reinforcing its potential as a principled approach for targeted attacks on complex networks. The consistently lower AUC values obtained with FGIA highlight its efficiency in dismantling structural cohesion with minimal interventions for the fact that FGIA method can remove only 5%-10% of the edges, effectively reducing the λ_2 of the network by about 90%. In the following sections, we extend this analysis to real-world networks to further validate FGIA’s effectiveness in practical applications.

Unsurprisingly, the superiority of FGIA is further validated across diverse real-world networks. The AUC metric, FGIA exhibits resilience dismantling capabilities across diverse real-world networks, as demonstrated by AUC metrics in Tab. I, quantifying the cumulative degradation of λ_2 , which consistently demonstrates FGIA’s unparalleled efficacy in suppressing resilience.

The results of our algorithm comparison in more real networks are shown in Tab. I. Similarly, we use AUC to characterize the attack effect of the algorithm. We mark

the smallest AUC value in red and the largest AUC value in blue. It is clear that the FGIA algorithm presents the best attack effect in all networks, and it is far ahead of other algorithms in most networks.

FGIA demonstrates a significant advantage across all six types of networks (e.g., brain networks, power systems, social networks, interaction networks, ecology networks and other networks) as shown in Tab. I. Across a total of 26 real-world network datasets[29], FGIA consistently achieves the lowest AUC among all compared algorithms, with an average reduction of 82.3% and a standard deviation of $\sigma = 7.1\%$. For instance, in the visual sub-network of the human brain, FGIA obtains an AUC of 0.020, which is 87.4% lower than the second-best algorithm, Eigenvector centrality based algorithm of 0.159, and is 91.8% lower than the worst algorithm, Betweenness centrality based algorithm of 0.243.

Analogously, the efficacy of compared algorithms in real-world network also vary significantly depending on network-specific characteristics. For example, betweenness centrality (Bet) shows relatively competitive performance in the rajat05 network in Fig. 6(e), while it fails to generalize to Human Brain-visual network in Fig. 6(a) or Ecology-everglades network in Fig. 6(d), even in a backward position. On the contrary, all the results highlight FGIA’s adaptability that its gradient-driven spectral analysis bypasses the limitations of topology-dependent heuristics, ensuring universal superiority regardless of network size, density, or functional context.

V. CONCLUSION

In this section, we further conclude the core of the Fiedler Gradient Iterative Attack (FGIA) algorithm. FGIA aims to dismantle the resilience of complex networks, where resilience is characterized by the convergence time of dynamic processes and quantified by the

TABLE I. AUC of different algorithms in real networks

Name	Node number(n)	Edge number(m)	FGIA	Deg	Bet	Clos	Eig	PR
Brain Network								
human-visual	111	1276	0.020	0.212	0.243	0.096	0.159	0.178
human-medial	172	2542	0.004	0.133	0.185	0.057	0.154	0.131
macaque-rhesus-cerebral-cortex 1	91	1401	0.009	0.111	0.139	0.106	0.077	0.123
macaque-rhesus-brain 2	91	582	0.152	0.609	0.613	0.491	0.502	0.626
mouse-visual-cortex 2	193	214	0.024	0.071	0.022	0.033	0.052	0.044
cat-mixed-species-brain 1	65	730	0.015	0.132	0.199	0.075	0.081	0.144
Power Networks								
power-494-bus	494	586	0.010	0.115	0.018	0.080	0.059	0.091
power-662-bus	662	906	0.007	0.098	0.077	0.076	0.062	0.111
power-bcspwr09	1723	4117	0.005	0.070	0.021	0.052	0.042	0.076
Social Networks								
soc-tribes	16	58	0.074	0.171	0.294	0.369	0.447	0.458
soc-karate	34	78	0.076	0.274	0.224	0.206	0.159	0.308
soc-dolphins	62	159	0.039	0.239	0.040	0.216	0.192	0.318
soc-pages-food	620	2102	0.018	0.310	0.019	0.232	0.298	0.311
Interaction Networks								
enron-only	143	623	0.016	0.348	0.041	0.204	0.100	0.428
crime-moreno	829	1476	0.002	0.156	0.149	0.060	0.113	0.156
Ecology Networks								
eco-stmarks	54	350	0.016	0.144	0.176	0.099	0.139	0.146
eco-everglades	69	880	0.009	0.125	0.162	0.087	0.091	0.131
eco-mangwet	97	1446	0.008	0.088	0.094	0.040	0.099	0.074
eco-florida	128	2075	0.007	0.224	0.268	0.073	0.262	0.254
eco-foodweb-baydry	128	2106	0.007	0.293	0.283	0.067	0.266	0.234
Other Networks								
road-Chesapeake	39	170	0.026	0.168	0.282	0.120	0.124	0.202
rajat05	301	668	0.008	0.088	0.065	0.104	0.044	0.100
insecta-ant-colony2-day37	58	928	0.009	0.028	0.177	0.648	0.658	0.693
ca-netscience	379	914	0.016	0.235	0.021	0.019	0.164	0.106
bio-celegansneural	297	2148	0.011	0.270	0.064	0.300	0.452	0.112
infect-hyper	113	2196	0.050	0.483	0.143	0.193	0.402	0.357

Fiedler value λ_2 . Since a higher λ_2 implies faster convergence and stronger resilience, reducing λ_2 effectively delays system recovery. FGIA leverages spectral perturbation theory to identify critical edges whose removal maximally decreases λ_2 . Specifically, it uses the gradient of the Fiedler vector, $\nabla_{\epsilon_{ij}} = |x_i - x_j|$, to evaluate each edge's importance, targeting those with the highest gradient magnitude for removal.

In conclusion, the Fiedler Gradient Iterative Attack (FGIA) algorithm offers an effective and computationally efficient approach for dismantling resilience in complex networks. By interpreting resilience through the lens of convergence time, quantified by the Fiedler value λ_2 , the method targets edges that contribute most to rapid system recovery.

FGIA combines hierarchical spectral bisection, Fiedler gradient-based edge ranking, and bridge detection to iteratively remove non-bridge edges while preserving global connectivity. It significantly outperforms conventional structural heuristics in reducing λ_2 , requiring fewer interventions to achieve comparable functional degradation. With a complexity of $O(n^3)$, it also achieves substantial efficiency gains over brute-force approaches with $O(n^6)$ complexity.

This work bridges theoretical insights from spectral graph theory with practical algorithms for network control, showing that resilience can be effectively suppressed through localized, informed edge removals. It highlights the potential of spectral-gradient-based analysis as a general tool for managing complex dynamical systems.

[1] S. H. Strogatz, Nature **410**, 268 (2001).

[2] X. Qi and G. Mei, Journal of King Saud University - Computer and Information Sciences **36**, 101882 (2024).

[3] S. Liu, B. Huang, and Y. Lin, Dynamics of Continuous, Discrete and Impulsive Systems. Series B: Applications and Algorithms (2024).

- [4] I. Belykh, M. Hasler, M. Lauret, and H. Nijmeijer, *Physical Review Letters* **94**, 188101 (2005).
- [5] K. A. H. Gerdes, M. A. Buice, and C. C. Chow, *Nature Communications* **14**, 3186 (2023).
- [6] T. Skowronski and C. Masoller, *Chaos: An Interdisciplinary Journal of Nonlinear Science* **33**, 053120 (2023).
- [7] V. Mathiopoulou, A. A. Kühn, A. Kupsch, B. Hellwig, G. Schneider, C. K. Moll, V. M. Tronnier, J. Volkmann, G. Deuschl, A. Kupsch, B. Hellwig, G. Schneider, C. K. Moll, V. M. Tronnier, J. Volkmann, and G. Deuschl, *Nature Communications* **16**, 1685 (2025).
- [8] J. Ruan, G. Fan, Y. Zhu, G. Liang, J. Zhao, and F. Wen, *IEEE Transactions on Smart Grid* **14**, 4035 (2023).
- [9] D. K. Mishra, J. Wang, L. Li, J. Zhang, and M. J. Hossein, *IEEE Transactions on Industrial Applications* **60**, 2277 (2023).
- [10] K. Y. Henry Tsang, B. Li, and K. Y. Michael Wong, in *Complex Networks and Their Applications VII*, edited by L. M. Aiello, C. Cherifi, H. Cherifi, R. Lambiotte, P. Lió, and L. M. Rocha (Springer International Publishing, Cham, 2019) pp. 854–865.
- [11] R. Olaniyan and M. Maheswaran, *IEEE Internet of Things Journal* **9**, 3825 (2022).
- [12] C. Chen, Z. Liu, Y. Zhang, C. P. Chen, and S. Xie, *IEEE Transactions on Cybernetics* **46**, 2311 (2015).
- [13] X. Pan, M. Zhang, D. Wu, Q. Xiao, S. Ji, and Z. Yang, in *29th USENIX Security Symposium (USENIX Security 20)* (2020) pp. 1641–1658.
- [14] M. Li, R.-R. Liu, L. Lü, M.-B. Hu, S. Xu, and Y.-C. Zhang, *Physics reports* **907**, 1 (2021).
- [15] U. Brandes, *Journal of Mathematical Sociology* **25**, 163 (2001).
- [16] R. Albert, H. Jeong, and A.-L. Barabási, *Nature* **406**, 378 (2000).
- [17] M. Fiedler, *Czechoslovak Mathematical Journal* **23**, 298 (1973).
- [18] F. Dörfler and F. Bullo, *Proceedings of the National Academy of Sciences* **110**, 2005 (2013).
- [19] F. Chen, J. Zhou, and J.-a. Lu, *International Journal of Bifurcation and Chaos* **34**, 2450142 (2024).
- [20] S. Jiang, J.-a. Lu, J. Zhou, and Q. Dai, *Physical Review E* **109**, 054301 (2024).
- [21] S. Jiang, J. Zhou, M. Small, J.-a. Lu, and Y. Zhang, *Physical Review Letters* **130**, 187402 (2023).
- [22] C. S. Holling, in *Engineering Within Ecological Constraints*, edited by N. A. of Engineering (The National Academies Press, Washington, DC, 1996) uRL: <https://nap.nationalacademies.org/read/4919/chapter/4>.
- [23] R. V. O’Neill, D. L. DeAngelis, J. B. Waide, and T. F. H. Allen, *A Hierarchical Concept of Ecosystems* (Princeton University Press, Princeton, N.J., 1986).
- [24] S. L. Pimm, *Nature* **307**, 321 (1984).
- [25] D. Tilman and J. A. Downing, *Nature* **367**, 363 (1994).
- [26] X. Liu, D. Li, M. Ma, B. K. Szymanski, H. E. Stanley, and J. Gao, *Physics Reports* **971**, 1 (2022).
- [27] J. Gao, B. Barzel, and A.-L. Barabási, *Nature* **598**, 45 (2021).
- [28] R. E. Tarjan, *SIAM Journal on Computing* **1**, 146 (1972).
- [29] R. A. Rossi and N. K. Ahmed, in *AAAI* (2015).